JACS
JOURNAL OF THE AMERICAN CHEMICAL SOCIETY

Article

Mediating K/H Transport on Organelle Membranes to Selectively Eradicate Cancer Stem Cells by a Small Molecule

Fang-Fang Shen, Sheng-Yao Dai, Nai-Kei Wong, Shan Deng, Alice Sze-Tsai Wong, and Dan Yang

J. Am. Chem. Soc., **Just Accepted Manuscript** • DOI: 10.1021/jacs.0c02134 • Publication Date (Web): 22 May 2020

Just Accepted

is published by the American Chemical Society. 1155 Sixteenth Street N.W., Washington, DC 20036

Mediating K^+/H^+ Transport on Organelle Membranes to Selectively Eradicate Cancer Stem Cells by a Small Molecule

Fang-Fang Shen, Sheng-Yao Dai, Nai-Kei Wong, Shan Deng, Alice Sze-Tsai Wong and Dan Yang*

ABSTRACT: Molecules that are capable of disrupting cellular ion homeostasis offer unique opportunities to treat cancer. However, previously reported synthetic ion transporters showed limited value as promiscuous ionic disruption caused toxicity to both healthy cells and cancer cells indiscriminately. Here we report a simple yet efficient synthetic K^+ transporter that takes advantage of the endogenous subcellular pH gradient and membrane potential to site-selectively mediate K^+/H^+ transport on the mitochondrial and lysosomal membranes in living cells. Consequent mitochondrial and lysosomal damages enhanced cytotoxicity to chemo-resistant ovarian cancer stem cells (CSCs) via apoptosis induction and autophagy suppression with remarkable selectivity (up to 47-fold). The eradication of CSCs blunted tumor formation in mice. We believe this strategy can be exploited in the structural design and applications of next-generation synthetic cation transporters for the treatment of cancer and other diseases related to dysfunctional K^+ channels.

INTRODUCTION

Ion transport proteins are located not only on the plasma membrane but also on organelle membranes. They exhibit unique ion and direction selectivity[1]. Major ions like K^+, Na^+, H^+, Ca^{2+} and Cl^- are distinctively distributed in cellular compartments to maintain electrochemical signals for physiological processes and support organelle functions. Small molecules that are capable of performing transmembrane ion transport have shown effectiveness in restoring ionic balance in disease models caused by defective ion transport proteins[2-5]. Disrupting normal ion homeostasis with ion transporters, on the other hand, was also demonstrated to be detrimental to cancer cells[6-8]. However, previous examples were less therapeutically valuable as they were cytotoxic to many types of cells indiscriminately[6]. Notably, different types of cells maintain subtly altered bioelectric properties, such as membrane potential, to regulate definite cell behaviors, including proliferation and differentiation[9]. Identify and selectively disrupt the critical electrochemical gradients may serve as a potential strategy to develop new cell-specific therapies.

K^+ channels are the largest ion channel family that is expressed in virtually all living organisms[10]. Ion flux across the subcellular organelle membranes constitutes over 80% of total ion transport processes. The major functions of organellar K^+ transport are to regulate osmotic homeostasis as well as to maintain membrane potentials[11]. Many K^+ transport processes inside cells are also coupled with H^+ or Ca^{2+} transport, which, in turn, regulate the pH levels within each compartment and control organellar functions governing metabolism, enzyme activity and protein secretion[12]. Growing evidence suggests that cancer cells, which show an abnormally high propensity to proliferate, are associated with K^+ channel dysregulation[13-14]. For instance, several types of human cancer cells including cancer stem cells (CSCs) have low expression of K^+ channels and hyperpolarized mitochondrial membrane potentials that contribute to apoptosis resistance[15-17]. Synthetic cation transporters that can modulate such gradients may serve as selective anticancer agents. Despite the fact that a considerable range of cation transporters have been reported, the majority of them are too large to be drug-like[18]. In addition, their transport activity studies were predominately restricted to *in vitro* characterization in liposomes[19-21]. It is thus challenging but imperative to develop active small molecules that could promote cation transport inside living cells.

To develop new synthetic cation transporters, we utilize α-aminoxy acids[22] as the main scaffold. Prior studies revealed that by incorporating two *α*-aminoxy acids into an isophthalamide unit, chloride channels[23] and chloride dependent potassium channels[24] can be formed via self-assembly. Yet, their transport activities were still unsatisfactory. Here we have performed structural modifications on α-aminoxy acid monomer to obtain a molecule with much smaller molecular weight but a drastically different mechanism and highly improved K^+ transport efficiency and selectivity.

RESULTS

Molecular design and ion transport mechanism. By conjugating *N*- and *C*-termini with benzoyl group and aniline, respectively, compound **1** was first synthesized from α-aminoxy O-benzyl-serine (Fig. 1a). K^+ transport activity of compound **1** was evaluated in large unilamellar vesicles (LUVs) prepared from egg yolk phosphatidylcholine (EYPC) encapsulating pH-sensitive dye 8-hydroxypyrene-1,3,6-trisulfonic acid (HPTS)[25]. The results shown in Figure 1b indicated poor K^+ transport activity of this compound. However, it was found that by modifying the *N*-terminal group to 3,5-bis(trifluoromethyl)benzoyl group, compound **2** exhibited significantly improved K^+ transport ability at the concentration of 10 μM. The *N*-terminal replacement may exert two effects that contribute to the improved K^+ transport activity. First, with the bis-CF_3 groups, the estimated Clog P value was increased from 3.4 (compound **1**) to 4.8 (compound **2**)[26], which corresponds to the improved lipophilicity and thereby better transmembrane K^+ transport activity[27]. Second, the electron-withdrawing effect of the bis-CF_3 substituents also increased the acidity of aminoxy amide NH. In addition, to confirm whether this acidic proton contributes to the K^+ transport, compounds **3**–**6** were synthesized. As shown in Figure 1b, once the acidic aminoxy amide proton was replaced with a methyl group (compound **3**), the K^+ transport activity vanished

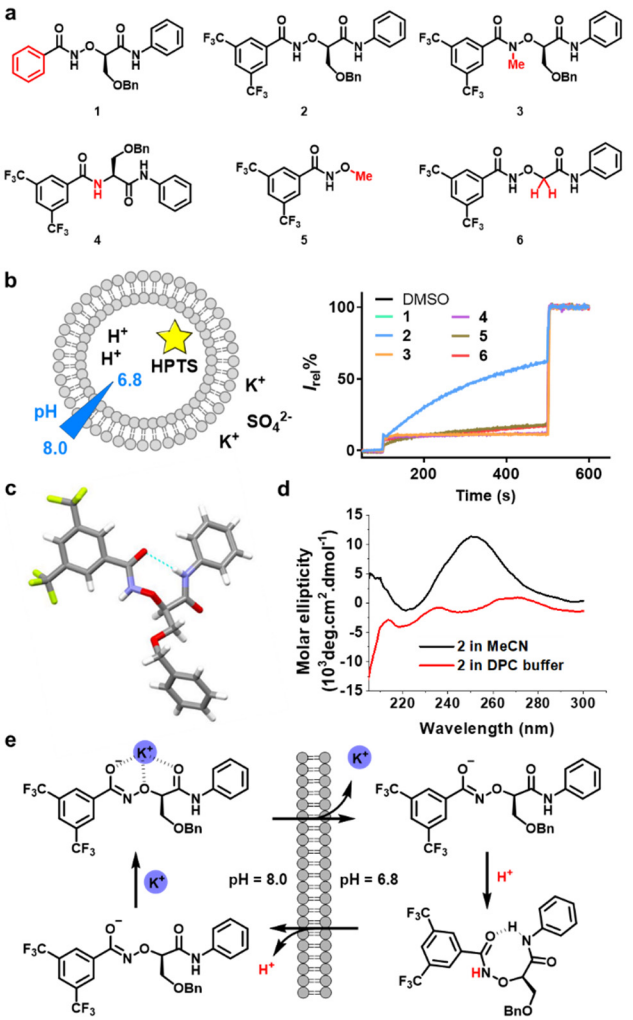

Fig. 1. Molecular design and transport mechanism studies. **a**, Chemical structures of aminoxy acid monomers **1**−**6**. **b**, K^+ transport behavior of compounds (10 μM) as evaluated by HPTS assay. **c**, X-ray crystallographic structure of compound **2**. All hydrogen atoms except N–H are omitted for clear presentation. Eight-membered ring hydrogen bond formation denotes the adoption of N–O turn conformation. **d**, CD spectrophotometer analysis of compound **2** (0.5 mM) in CH_3CN (black) and 50 mM DPC (red) at pH 7.4. **e**, Proposed transport mechanism of compound **2** in liposome assays.

completely. Similarly, without α-effect from the extra oxygen atom, compound **4** that was built from amino acid serine exhibited no K^+ transport activity. These results indicated the critical roles of free aminoxy amide NH for K^+ transport. The K^+ transport capacity was also significantly reduced when the molecule was truncated (compound **5**) or when the side chain was completely removed (compound **6**). The X-ray crystallographic structure of compound **2**, crystallized in ethyl acetate and hexane, confirmed the existence of the anticipated N–O turn in the solid state[28-29] (Fig. 1c), which was also supported by circular dichroism (CD) spectra obtained in acetonitrile (Fig. 1d). However, the CD spectrum of compound **2** obtained in dodecylphosphocholine (DPC) buffered at pH 7.4 clearly showed the loss of its secondary structure. We hypothesized that the bis-CF_3 substituted aminoxy amide NH group is partially deprotonated at physiological pH. Indeed, the pK_a of aminoxy NH group was found to decrease from around 8.3 to around 7.1 upon the bis-CF_3 substitution (Fig. S1). In our liposome assays, the extravesicular pH value was maintained at around 8.0, at which the predominant population of compound **2** would be the anionic form.

To fully understand the transport mechanism, further studies were performed. According to the previously reported method[30], ^{39}K NMR technique was used to study the K^+ binding stoichiometry (Fig. S2). The calculated transport rate (see method) varied linearly with the compound concentration in LUVs containing different concentrations of K^+ (75 mM, 100 mM and 125 mM) (Fig. S3). This result strongly indicated the formation of a 1:1 complex between K^+ and compound **2** during transmembrane transport.

Supported by the structure-activity relationship study, it is highly likely that compound **2** transports K^+ through a 1:1 carrier mechanism. In the anionic form, it could bind to K^+ through electrostatic interaction as well as chelation, possibly by aminoxy oxygen atom and the two carbonyl groups. In addition, the hydrophobic sidechain OBn group and the *N*- and *C*-terminal substituents might shield the hydrophilic K^+ ion during transport. After entering into liposomes, where the intravesicular pH value was around 6.8, compound **2** can be re-protonated and release K^+ ion. Compound **2** in neutral form can freely diffuse through the membrane to complete the carrier cycle (Fig. 1e).

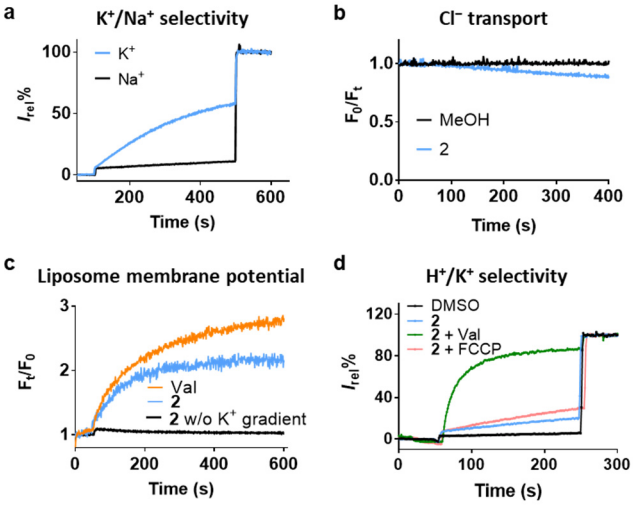

Fig. 2. Ion transport activities of compound **2**. **a**, K^+/Na^+ selectivity of synthetic K^+ transporter **2** at a concentration of 10 μM. **b**, Cl^- transport activity of compound **2** as evaluated by SPQ assay. **c**, Liposome membrane potential as evaluated by safranin O assay. Val was used as a positive control. All the molecules were used at the final concentration of 1 μM. **d**, Ion transport activity of compound **2** (0.3 μM) in the presence or absence of the proton ionophore FCCP (100 nM) or the potassium ionophore Val (25 nM).

Selective K^+ and H^+ transport in liposomes. Next, the ion selectivity of compound **2** was further evaluated in liposome assays (see details in Methods). It was found that compound **2** exhibited excellent K^+/Na^+ selectivity but did not transport Cl^- (Figs. 2a and 2b) with EC_{50} values of 2.02 μM (4.04 mol%) for K^+ and 47.26 μM (94.52 mol%) for Na^+, respectively (Figs. S4−S8). The EC_{50} values of compound **2** for different ions and K^+/Na^+ selectivity were summarized in Table 1. The selectivity of compound **2** towards other alkali metal cations was also evaluated (Fig. S9). Compound **2** has shown a selectivity trend of $K^+ > Cs^+ > Li^+ > Na^+$ in the presence or absence of pH gradient, which implied that the transport ability was not directly correlated with dehydration energy or sizes of ions[31]. Compound **2** with remarkable K^+ selectivity was able to establish stable membrane potential in safranin O assay[32] at a concentration of 1 μM, which was comparable to that of natural potassium ionophore valinomycin (Val) (Fig. 2c). At a concentration of 10 μM, no carboxyfluorescein release was detected, suggesting the absence of pore formation in lipid bilayers (Fig. S10).

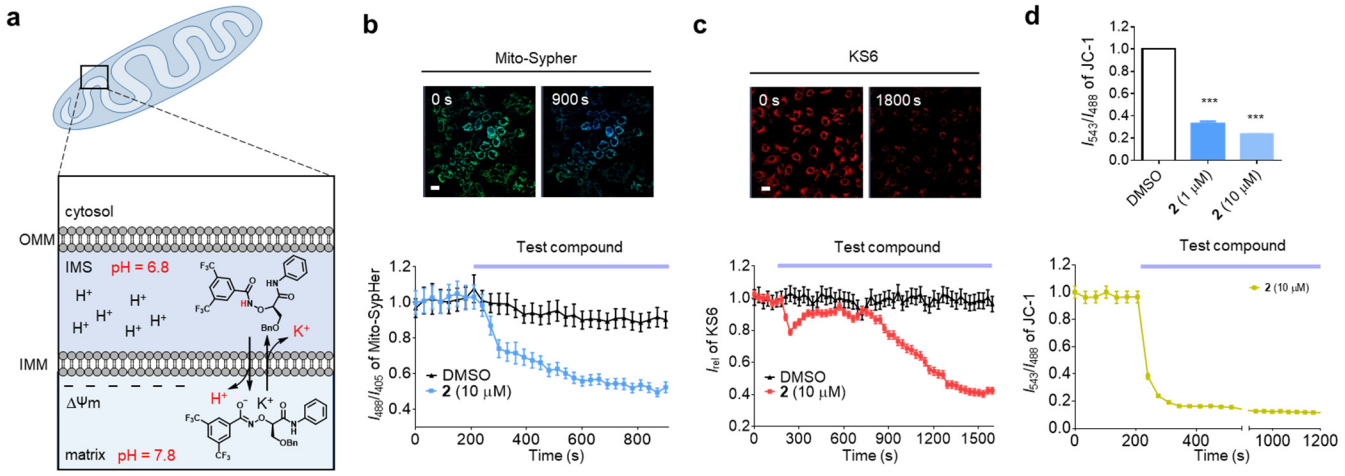

Fig. 3. Selective K^+/H^+ transport on the inner mitochondrial membrane. **a,** Illustration of the transport behavior of compound **2** in the context of mitochondria. **b**, Representative confocal images and quantitative fluorescence measurements representing kinetic changes in matrix pH of HeLa cells (n = 10−20 cells) transfected with Mito-SypHer. Compound **2** was added at 180 s (mean ± s.e.m., n = 20−30 cells). **c**, Representative confocal images and quantitative fluorescence measurements of mitochondrial-targeting K^+ probe KS6 representing kinetic changes in matrix K^+ concentration in SKOV3 cells. Compound **2** was added at 180 s (mean ± s.e.m., n = 20−30 cells). **d**, Quantification of measurements of mitochondrial membrane potential using probe JC-1 in HEYA8 cells treated with compound **2** for 10 min (mean ± s.e.m., n = 20−30 cells, ***p < 0.001, one-way ANOVA) and kinetic changes in mitochondrial membrane potential of HEYA8 cells. Compound **2** was added at 180 s (mean ± s.e.m., n = 20−30 cells). Scale bars denote to 20 μm.

To identify relative K^+/H^+ transport of compound **2**, the HPTS assay was performed in the presence of Val and carbonyl cyanide-4-(trifluoromethoxy)phenylhydrazone (FCCP) to counter-balance the rate-limiting ion[33]. As shown in Fig. 2d, a significant increase in HPTS fluorescence by compound **2** was observed in the presence of Val but not FCCP. This suggested that compound **2** was an electrogenic transporter with a $H^+ > K^+$ transport rate. This result further confirmed our model that compound **2** can facilitate the movement of both K^+ and H^+ down their electrochemical gradients independently. In the presence of Val, the EC_{50} value of proton transport activity was determined to be 0.15 μM (0.30 mol%) (Fig. S11).

Table 1. Summary of ion transport activities of compound 2.

EC_{50} (mol%)			EC_{50} K^+/Na^+	R_{K^+}/R_{Na^+}	Hill coefficient		
K^+	Na^+	H^+			K^+	Na^+	H^+
4.04[a]	94.52[b]	0.30[c]	23.4	16.0[d]	0.84[a]	3.66[b]	1.41[c]

EYPC vesicles encapsulating 75 mM K_2SO_4 were suspended in [a]75 mM K_2SO_4 buffer, or [b]75 mM Na_2SO_4 buffer. [c]Tested in the presence of 25 nM Val in 75 mM K_2SO_4 buffer. [d]Ratio of fractional transport activity (see Fig. S8).

Selective K^+/H^+ transport on the inner mitochondrial membrane. We thus asked whether compound **2** could promote ion transport in living cells. We first investigated the changes of cytosolic K^+ concentration and the plasma membrane potential in human ovarian cancer HEYA8 cells. Following the treatment with compound **2**, however, no significant ion transport across the plasma membrane was detected (Figs. S12 and S13).

Mitochondria are double-membrane organelles, composed of the inner membranes (IMM) and outer membranes (OMM). During oxidative phosphorylation (OXPHOS), the electron transport chain complexes located on IMM pumped protons out from the matrix to the intermembrane space (IMS), which generates the mitochondrial membrane potential (ΔΨm) and pH gradient with higher pH level in the matrix (pH ≈ 7.8) than that in the cytosol (pH ≈ 6.8)[34]. In mitochondria, the pH gradient and ΔΨm would act as strong driving forces for compound **2** to facilitate K^+ and H^+ transport across IMM. We speculated that the neutral form of compound **2** could freely pass through IMM and enter the matrix, where it subsequently loses one proton and changes to the anionic form. Due to the negative charges on IMM, this anionic form could be trapped in the matrix, unless it forms a neutral complex with one K^+ and travels back to the intermembrane space. This cycle would lead to H^+ and K^+ exchange in the matrix (Fig. 3a).

To confirm this hypothesis, matrix pH change was monitored by real-time confocal imaging in HeLa cells transfected with the pH-sensitive mitochondria-targeted fluorescent protein Mito-SypHer[35] (Fig. 3b and S14a). Upon addition of compound **2**, a spontaneous decrease in the green to blue fluorescence ratio (I_{488}/I_{405}) was observed, suggesting that matrix H^+ influx was induced. This effect was also confirmed in human ovarian cancer SKOV3 cells (Fig. S14b). Matrix K^+ concentration was also monitored by a mitochondria-targeting K^+ fluorescent probe KS6[36]. An obvious drop in fluorescence intensity of KS6 occurred in SKOV3 cells shortly after the addition of compound **2**, which indicated K^+ efflux (Figs. 3c and S15). As ΔΨm was closely related to ionic balance, we next monitored its change with a ratiometric fluorescent probe JC-1. A decreased red to green fluorescence ratio of JC-1 was observed in live-cell confocal imaging, in a dose-dependent manner, indicating ΔΨm dissipation (Figs 3d and S16). Kinetics studies demonstrated that an acute depolarization of ΔΨm occurred within 30 s upon compound **2** addition, which suggested the faster rate of H^+ influx in the matrix than that of K^+ efflux. This H^+ influx and K^+ efflux processes on IMM agreed well with our hypothesis and the characterized transport activity of compound **2** in liposomes.

Disruption of mitochondrial functions. Given that ion homeostasis is coupled to mitochondrial functions[37], we further evaluated the acute effects of compound **2** on mitochondrial ROS production[38], respiration and mitochondrial morphology in HEYA8 cells. Mitochondrial superoxide ($O_2^{\bullet-}$) production was monitored with the chemoselective fluorescent probe HKSOX-2m[39]. A surge in $O_2^{\bullet-}$ level occurred shortly after the challenge of cells with compound **2** (Figs. 4a and S17). Disturbance to K^+/H^+ homeostasis induced by cation transporter **2** also significantly dampened mitochondrial respiration. As illustrated in the oxygen consumption rate (OCR) assay (Fig. 4b), following the addition of oligomycin (ATP synthase inhibitor), compound **2** (10 μM) caused an immediate rise

in OCR of intact HEYA8 cells. This was due to the collapse of the proton gradient, which allowed the oxygen consumption of complex IV to reach the maximum. Subsequently, cells treated with compound **2** showed no respiratory response to FCCP. These results corroborated the notion that our K^+ transporter drastically impairs cell respiration through the dissipation of pH gradient across IMM[40]. Homeostasis of K^+ and H^+ is essential for maintaining the matrix volume and structural integrity of mitochondria[12, 37]. Therefore, we examined mitochondrial morphology in HEYA8 cells treated with compound **2**. Upon 1 h incubation, mitochondria underwent a morphological change into a round shape, in contrast to their characteristic tubular morphology in resting cells, suggesting a stress induction (Fig. 4c). As a whole, these results indicated that K^+ and H^+ transport across IMM mediated by compound **2** coordinately resulted in the damage of mitochondrial functions.

Selective killing of salinomycin resistant ovarian CSCs. CSCs, as a minor cell subpopulation in tumors, are resistant to many current therapies and privileged with the capacity for self-renewal, which leads to tumor relapse and poor prognosis[41]. Selective elimination of CSCs has been proposed as a promising direction to improve current anti-cancer treatments[42-43]. Accumulating evidence suggests that many CSCs, including ovarian CSCs, are

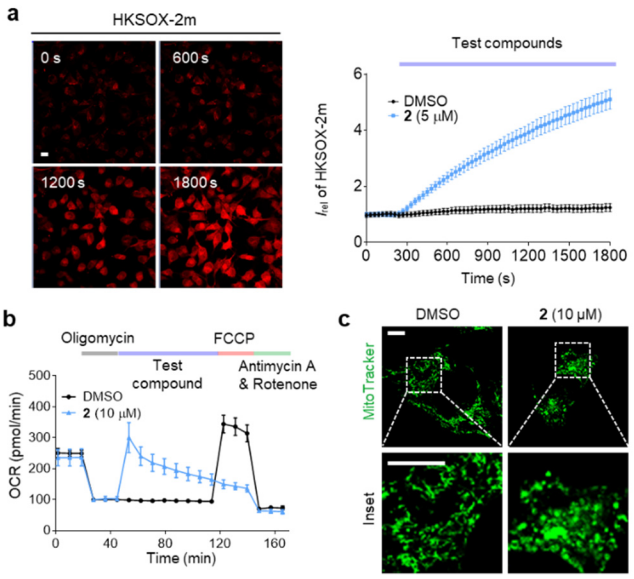

Fig. 4. Synthetic cation transporters perturbed mitochondrial functions. **a**, Representative confocal images and quantitative fluorescence measurements of mitochondrial superoxide levels in HEYA8 cells stained with HKSOX-2m (4 μM). Scale bars = 20 μm. Compounds at a final concentration of 5 μM were added at 180 s (mean ± s.e.m., n = 20−30 cells per group). **b**, OCR as measured by the Seahorse instrument (mean ± s.e.m., n = 3). **c**, Representative confocal images for analysis of mitochondrial morphology of MitoTracker Green-stained HEYA8 cells treated with compound **2** (10 μM) for 1 h. Scale bars = 10 μm.

characterized by hyperpolarized ΔΨm, due to the oxidative phosphorylation (OXPHOS)[16] dependence. The dissipation of ΔΨm thus provides a viable strategy in selective eradication of CSCs[44]. Salinomycin, a natural polyether K^+ ionophore, was previously identified as the leading anti-CSCs agent[45-46]. However, emerging evidence suggested that CSCs overexpressing ATP-binding cassette transporters (ABC transporters), as in the case of ovarian cancer[47], are non-susceptible to salinomcin[48]. With our synthetic transporter **2**, we next tested the effect of K^+/H^+ transport on drug-resistant ovarian CSCs. We utilized the CSC model of ovarian SKOV3 and HEYA8 cells previously established by sphere-forming in non-adherent, stem-cell-selective conditions (Fig. 5a)[49]. An enriched population of cells with $CD133^+$ antigenic phenotype representing ovarian CSCs[50] was confirmed in spheres (Fig. 5b). Consistent with literatures[51-52], increased mitochondria mass (Fig. S18) and hyperpolarized mitochondria membrane potential were detected (Fig. S19) in CSCs. When the CSCs were treated with compound **2**, depolarization of mitochondria was clearly observed even when the concentration was as low as 200 nM (Fig. S20). These results were consistent with our previous studies in adherent cancer cells and suggest that the ion transport activity of compound **2** was conserved in CSCs.

It was found that compound **2** inhibited the growth of CSCs at a concentration of 5 μM, which was otherwise non-toxic to adherent cancer cells (Fig. 5c). Other non-transporting compounds **1**, **3**, **4**, **5** and **6**, on the other hand, did not show significant toxicity at the same dose. Known resistance to paclitaxel (PTX) in these ovarian CSCs was also observed. Interestingly, Val and FCCP, which solely transport K^+ and H^+, respectively, showed lower toxicity toward CSCs than cancer cells. Comparisons of IC_{50} values of K^+ transporter **2**, salinomycin and nigericin against ovarian CSCs and cancer cells were shown in Figs. 5d and 5e. Compound **2** displayed high selectivity towards ovarian CSCs and only moderate toxicity towards adherent cancer cells and noncancerous cells (HEK293, NIH3T3, and MDCK) (Fig. S21, Table 2). This selectivity was found to be as high as 47-fold in the case of the IC_{50} of compound **2** towards SKOV3 CSCs and corresponding cancer cells. In contrast, the CSCs were resistant to both salinomycin and nigericin (Figs. 5d,e) due to their abundant expression of ABC transporters (ABCB1 and ABCG2)[47] (Fig. S22). When HEYA8 cells were treated with compound **2**, the proportions of $CD133^+$ subpopulation declined (Fig. 6a). In contrast, PTX treatment increased this subpopulation. As an *in vitro* measurement of CSC activity, we tested the ability of cells to form spheres when grown in suspension cultures. In agreement with the above results, significantly fewer spheres were observed in cells treated with compound **2** (Fig. 6b). As a functional assessment of CSC inhibition, an *in vivo* tumor-forming experiment was performed. Cells were pretreated *ex vivo* with compounds for 2 days, then were allowed to recover for 10 days before injected subcutaneously into nude mice. This experiment allows direct evaluation of the subsequent *in vivo* tumor-forming ability of the treated cells. The recovery period is critical, as it ensures tumor-forming ability is directly correlated to CSC population among the cells but not due to the loss of viability. It was found that cells pretreated with compound **2** showed significantly decreased ability in tumor formation than the untreated cells or those treated with PTX (Fig. 6c). Moreover, compound **2** itself could also reduce the size of established tumor in nude mice model (Fig. S23). Collectively, our results demonstrated that K^+/H^+ transport on the inner mitochondria membrane can lead to selective eradication of ovarian CSCs.

Induction of apoptotic cell death and suppression of autophagy. Mitochondrial oxidative stress and ΔΨm dissipation are considered critical pro-apoptotic events to initiate mitochondria-mediated (intrinsic) apoptotic cascades characterized by the activation of caspases-9, caspase-3[53] and subsequently poly [ADP-ribose] polymerase 1 (PARP-1)[54]. It was found that after 48 h treatment with compound **2**, a much higher proportion of apoptotic cells were detected in CSCs than in cancer cells, even when CSCs were treated with 10-fold lower concentrations (Fig. 7a). Immunoblot showed that cleavage of procaspase-9, -3 and PARP-1 were detected in CSCs treated with transporter **2**, which indicated mitochondria-mediated apoptosis (Fig. 7b). Depolarization of ΔΨm would initiate mitophagy through the PINK1/Parkin pathway[55]. Following treatment with compound **2** for 2 h, merging of mitochondria (green) and lysosomes (red) was observed in HEYA8 cells. These observations serve as an early sign of mitophagy to

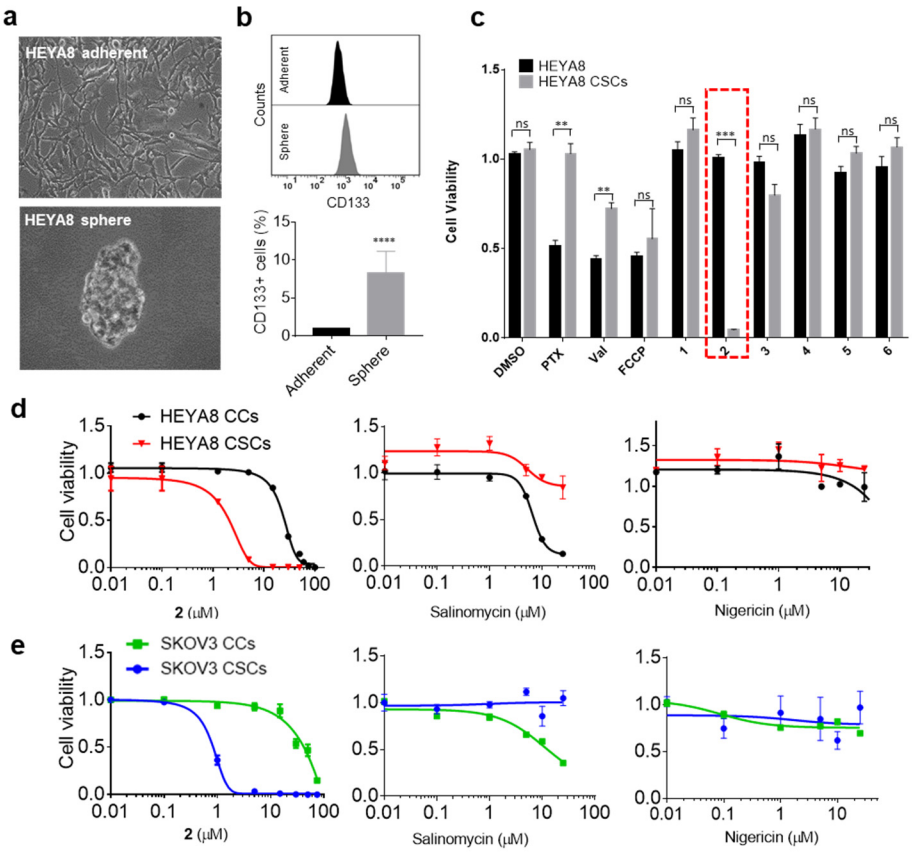

Fig. 5. Synthetic cation transporters selectively killed ovarian CSCs. **a**, Microscopic images of HEYA8 cells cultured as spheres and adherent cells. **b**, HEYA8 cells cultured as spheres had higher proportions of CD133$^+$ antigenic phenotype (mean ± s.e.m., $n = 3$, ****p <0.001). **c**, Viability of HEYA8 cancer cells and CSCs following treatment of PTX (100 nM), Val (5 μM), FCCP (5 μM), compounds **1**–**6** (5 μM) for 48 h (mean ± s.e.m., $n = 3$, **$p < 0.01$, ***$p < 0.001$). **d**, **e**, Representative viability curves of HEYA8 and SKOV3 cancer cells and CSCs following treatment of compound **2**, salinomycin, or nigericin for 48 h (mean ± s.e.m., $n = 3$).

Table 2. Summary of IC_{50} values (μM) of compound 2 on cancer cells, CSCs, and non-cancer cells.

HEYA8		HEYA8 CSCs selectivity	SKOV3		SKOV3 CSCs selectivity	HEK293	MDCK	NIH3T3
Sphere	Adherent		Sphere	Adherent		Non-cancer Cells		
1.5 ± 1.3	23.4 ± 2.1	16-fold	0.9 ± 1.0	42.1 ± 5.2	47-fold	51.0 ± 1.0	25.1 ± 1.1	30.5 ± 1.1

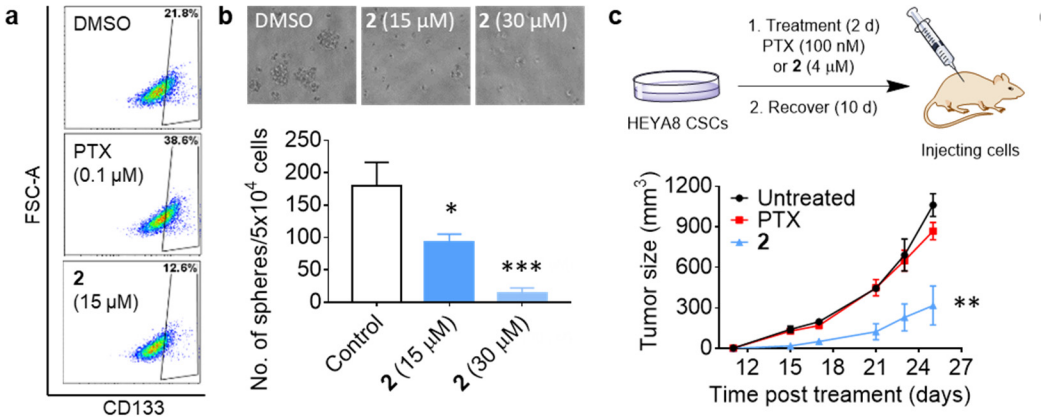

Figure 6 Synthetic cation transporters reduces CSCs population *in vitro* and tumor-forming ability *in vivo*. **a**, *In vitro* effects of PTX (100 nM) or compounds **2** (15 μM) against CD133$^+$ HEYA8 cell population following treatment for 72 h. Fluorescence for PE-conjugated anti-CD133 antibody was measured by flow cytometry. **b**, Sphere-forming ability of HEYA8 cells following treatment as indicated for 48 h (mean ± s.e.m., $n = 3$, *$p < 0.05$, **$p < 0.01$, ***$p < 0.001$). **c**, *In vivo* tumor forming ability of HEYA8 CSCs treated as indicated (mean ± s.e.m., $n = 4$ mice per group, **$p < 0.01$).

indicate the fusion of autophagosomes with lysosomes[56] (Fig. 7c). Next, protein levels of the autophagy components, i.e. microtubule-associated protein light chain 3 (LC3) and p62, were monitored by immunoblotting. Upon treatment with compound **2** for 24 h, the conversion of LC3-I to LC3-II was detected in both HEYA8 adherent cancer cells and CSCs in a dose-dependent manner (Fig. 7d), suggesting the initiation of autophagy. However, the upregulation of both LC3-II and p62 implies the suppression of subsequent proteolytic degradation. Again, the effects of compound **2** were more profound in CSCs.

We expected that the pH gradient existing between the cytosol and lysosomal lumen (pH 4.5–4.7) also provides a driving force for ion transport across lysosomal membranes (Fig 7e). As shown in Figure 7f, significantly decreased red fluorescence of lysosome pH sensor acridine orange (AO) was observed in HEYA8 cells 1 h after the addition of compound **2**, which illustrated the pH increase of lysosomes was caused by proton efflux from lysosomes. The lysosome alkalization induced by compound **2** was likely to inhibit further proteolytic degradation process[57]. Altogether, we have demonstrated that K^+/H^+ transport induced by compound **2** on mitochondrial and lysosomal membranes act coordinately to selectively induce apoptotic cell death and suppress autophagy of ovarian CSCs.

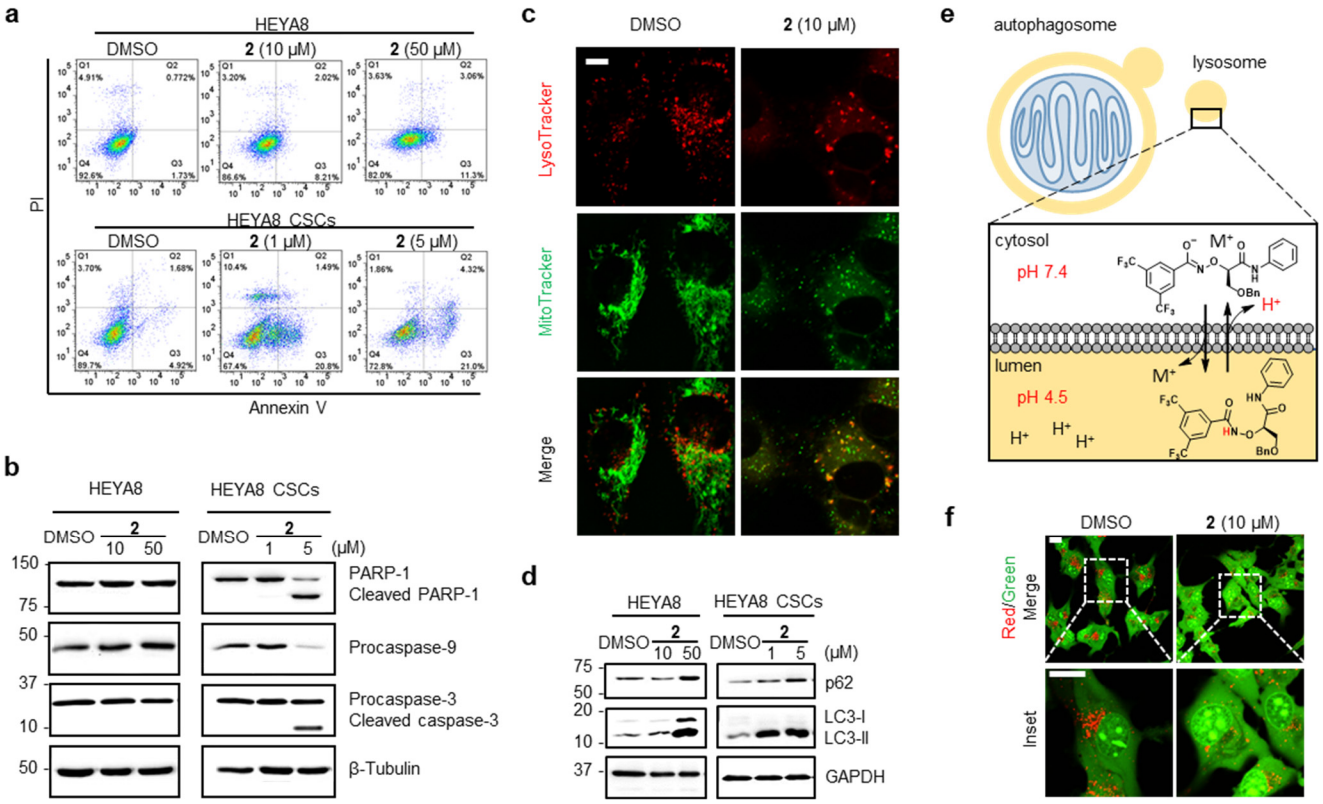

Fig. 7. Synthetic compound **2** induced apoptosis and suppressed autophagy in HEYA8 cancer cells and CSCs. **a**, Flow cytometry analysis of apoptosis in HEYA8 ovarian cancer cells and CSCs following indicated treatment for 48 h. Data were acquired immediately after cells were stained with Annexin V-Alexa 488 and propidium iodide (PI). **b**, Immunoblots showing the levels of PARP-1, cleaved PARP-1, procaspase-9, procaspase-3, cleaved caspase-3 and β-tubulin (internal loading control) in HEYA8 cells following indicated treatment for 48 h. **c**, Representative confocal images for analysis on co-localization of lysosomes (stained with LysoTracker Red) and mitochondria (stained with MitoTracker Green) in HEYA8 cells treated with compound **2** (10 μM) for 2 h. Scale bar = 10 μm. **d**, Immunoblots showing the levels of p62, LC3-I, LC3-II and GAPDH (internal loading control) in HEYA8 cells following indicated treatment for 24 h. **e**, Illustration of the transport behavior of compound **2** in the context of lysosomes. **f**, Representative confocal images of lysosomal pH probe acridine orange in HEYA8 cells treated with compound **2** (10 μM for 1 h). Scale bars = 20 μm.

DISCUSSION

Disrupting ion homeostasis with synthetic ion transporters has been demonstrated to cause cell death. However, this approach has shown limited clinical potential in cancer treatment as the resulting ionic disruption would cause toxicity to cancer cells and normal cells indiscriminately[58]. As different types of cells establish altered ionic regulation to maintain their distinct physiology, we have successfully demonstrated that targeting these critical electrochemical gradients can serve as a promising strategy to attack cells selectively.

In this study, we have developed a simple yet efficient synthetic ion transporter, compound **2**, which could selectively mediate K^+/H^+ transport in living cells. It is found that compound **2**, without bearing any organelle-targeting moieties, could site-selectively function on the mitochondrial and lysosomal membranes within minutes upon addition. Our mechanistic studies have revealed that compound **2** allows ion transport to take place in the above-mentioned sites by exploiting endogenous subcellular proton gradients and membrane potential. The localized K^+/H^+ flux potently disrupted mitochondrial and lysosomal functions, which are characterized by the dissipation of mitochondrial membrane potential, ROS production, uncoupling of respiration, mitochondrial morphological changes and pH alterations in lysosomes. All these effects culminated in up to 47-fold selectivity in killing ovarian CSCs via apoptosis induction and autophagy suppression. The selective depletion of CSCs by compound **2** also blunted tumor formation in mice. The exceptionally enhanced cytotoxicity of compound **2** towards ovarian CSCs was ascribed to the higher dependence of those CSCs on OXPHOS in mitochondria for energy production[16].

In contrast, cancer cells favor the glycolysis pathway for metabolism that is known as the "Warburg effect". Our results are in line with the recent findings that ovarian CSCs are more sensitive towards extrinsic inducers of mitochondrial stress and damage in triggering apoptosis[59]. It has also been reported that autophagy is essential for CSCs' self-renewal capacity and pluriopotency[60]. The suppressed autophagy processes as a result of lysosome alkalization induced by compound **2** also contributed to its selective cytotoxicity towards ovarian CSCs.

Previously, salinomycin was identified as the leading anti-CSCs agent[45]. As a well-known potassium ionophore, salinomycin has also been demonstrated to facilitate K^+/H^+ exchange across the inner mitochondrial membrane[40]. It is possible that the K^+/H^+ transport behavior of salinomycin acts as the upstream effect that directs to the intricate cell responses for selective CSCs killing[61-64]. Since emerging evidences have challenged the therapeutic potential of salinomycin due to drug extrusion by ABC transporters[48], the use of our newly developed molecule to induce K^+/H^+ transport could guide us to achieve more potent, less toxic and resistance-evasive therapies for CSCs elimination.

Our studies have also introduced a novel strategy for the development of synthetic small-molecule K^+ transporter. Building synthetic molecules that could mimic the function of K^+ channels has attracted intensive interests. Despite the extended efforts, the majority of the prior examples were constructed with complex scaffolds, such as oligophenyl rods[18], calix[4]arene[65], pillar[n]arene[66], and cyclic peptides[67-68] Recently, by using crown ether as cation binding unit, several small-molecule K^+ transporters have also been reported[32, 69]. However, the ion transport activities of all those reported molecules were constrained to *in vitro* characterization in liposomes. The therapeutic values of synthetic cation transporters have been underexplored. Here, by using α-aminoxy acids as a novel K^+ recognition scaffold, a simple K^+ transporter with excellent transport efficiency and K^+/Na^+ selectivity was constructed. It was found that the increased acidity of aminoxy amide NH allowed compound **2** to partially adopt anionic form in physiological pH (7.4), which enabled its binding with K^+ through electrostatic interaction and chelation. Other hydrophobic moieties of the molecule, including the side chain, the *N*- and *C*-terminal carbonyl groups, shielded the hydrophilic cation to lower the physical barriers during the diffusion through membrane lipids. However, attempts to measure the K^+ binding by using UV/vis spectroscopy, isothermal titration calorimetry and ^{1}H NMR methods failed, as negligible change was observed with KPF_6 titration, in either acetonitrile or dodecylphosphocholine (DPC) micelles (data not shown). These results indicated–relatively weak cation binding affinity for compound **2**, suggesting that tight association with cation may not be necessary for transport, instead, suitable initial cation recognition and hydrophobicity should be more critical in efficient transmembrane movement. We anticipate that further studies could enable us to define in more detail the structural underpinnings of K^+/Na^+ selectivity of aminoxy acids. We believe this insight could further guide the development of small yet more selective and efficient cation transporters into improved therapeutics.

More broadly speaking, our discoveries of small molecule-based K^+ transporter would also foster the development of new therapies for other diseases related to dysregulation of K^+ channels, such as long QT syndrome, neuronal disorders, and Alzheimer's disease, arise from potassium channel deficiency and cause erratic potassium gradient build-up across compartment-specific membranes[70]. By understanding and harnessing the properties of such ion gradients, small cation transporters with the capacity to autonomously perform K^+ movement have the potentials to restore such K^+ accumulation and treat diseases.

CONCLUSIONS

In summary, a novel small-molecule K^+/H^+ transporter, compound **2**, was developed by using an α-aminoxy acid monomer. By disturbing the critical mitochondrial and lysosomal ionic gradients in cells, this molecule exhibits exceptional selectivity in killing drug-resistant ovarian CSCs. We believe the structural and biological insights from our study could guide the design, optimization and application of small-molecule synthetic cation transporters as well as other small molecules that selectively eradicate cancer stem cells.

Methods

Base-pulsed HPTS assay. HPTS-loaded LUV suspension (100 μL) prepared as described above was added in isotonic HEPES buffer (1.9 mL) and placed into a fluorometric cuvette. HPTS fluorescence was monitored with excitation at 403 and 460 nm, and emission at 510 nm. At t = 100 s, DMSO solution of the test compounds (20 μL) and 0.5 M NaOH/KOH aqueous solution (20 μL) were added through an injection port. Addition of the base caused about 1 pH unit increase in the extravesicular buffer. At t = 500 s, 40 μL of 5% Triton X-100 was added to lyse the liposomes. The fluorescence ratio of F460/F430 of initial 100 s was set as 0% ion transport and the final fluorescence ratio of F460/F430 induced by Triton X-100 was set as 100% ion transport. DMSO or other solvents as indicated was used as control.

Cancer stem cell cultures. Isolation and culture of spheres were performed in serum-free stem-cell-selective condition as described in literature[49]. Briefly, 1–2 weeks after seeding, non-adherent spherical clusters of cells could be observed and were separated from single cells by low-speed centrifugation. After 8th to 10th passages, the non-adherent spherical clusters of cells appeared as distinct spheres. Using this selection condition, HEYA8 spheres (HEYA8 CSCs) could be enzymatically dissociated and reformed into spheres within 3 days under stem-cell-selective condition. To allow differentiation, dissociated sphere cells were plated on tissue culture plates in medium (MCDB 105: M199 = 1:1) supplemented with 10% FBS and 1% penicillin-streptomycin. The culturing methods for other types of cells including MDCK, HEK293 and NIH3T3 are provided in the Supplementary Information.

Measurement of adherent cell viability. Cells were plated in triplicate in 0.1 mL full medium in 96-well plates for 24 h. After that, the medium was changed to the freshly prepared medium with various concentrations of the test compound. Cells were incubated for another 48 h. Then the cell viability was measured by CellTiter-Glo® Luminescent Cell Viability reagent according to the manufacture's instruction. The luminescence at 550 nm was measured using a microplate reader (DTX 880 Multimode Detector, Beckman Coulter). Data were analyzed by GraphPad software 7.00.

Measurement of CSCs viability. HEYA8 or SKOV3 CSCs (5×10^4) were plated in triplicate in 10 mL serum-free MCDB105 medium in a 100-mm Petri dish for 7 days to form spheres. Then test compounds at different concentrations were added. The cells were further incubated at 37°C for 48 h. After that cells were collected by centrifugation and the medium was removed. Then 100 μL of CellTiter-Glo® Luminescent Cell Viability reagent was added into each tube, which was incubated for 10 min with shaking. After that, the reagent was transferred into 96-well plates and cell viability was measured using a microplate reader (DTX 880 Multimode Detector, Beckman Coulter).

Oxygen consumption rate assay. Cell respiration was measured by using an XF24 Extracellular Flux Analyzer (Seahorse, Bioscience), which measures the oxygen consumption rate (OCR). Adherent HEYA8 cells were seeded at 50000 cells/well in 200 μL of their culture medium and incubated for 24 h at 37°C in a humidified

atmosphere with 5% CO_2. The medium was then replaced with 670 μL/well of high-glucose DMEM without serum and supplemented with 1 mM sodium pyruvate and 2 mM L-glutamine. The oxygen consumption rate (OCR) was measured with an extracellular flux analyzer (Seahorse) at preset time intervals upon the preprogrammed additions of the following compounds: oligomycin to 1 μM, FCCP to 500 nM, antimycin A and rotenone to 0.5 μM final concentrations.

Measurement of the *in vivo* tumor-forming ability. All animal experiments were approved by the Committee on the Use of Live Animals in Teaching and Research (CULATR) at the University of Hong Kong. *In vivo* tumor-forming ability of cells after treatment with compound **2** was evaluated. Paclitaxel was used as a negative control. For this experiment, HEYA8 CSCs were pretreated with **2** (4 μM) or paclitaxel (0.1 μM) for 2 days in a suspension medium, respectively. Then cells were allowed to proliferate in full medium in the absence of drugs for 10 days. After that, 10^6 cells were subcutaneously (s.c.) injected into the flank of athymic nude mice bilaterally. The length and width of a tumor were measured with a caliper for 25 days after injection and tumor volume was calculated as Tumor volume $V = (\pi \times L \times W^2)/6$, where L represents the largest tumor diameter and W represents the perpendicular tumor diameter.

ASSOCIATED CONTENT

Supporting Information. Full experimental details are given in the Supplementary Information.

AUTHOR INFORMATION

Corresponding Author

Dan Yang – *Morningside Laboratory for Chemical Biology, Department of Chemistry, The University of Hong Kong, Pokfulam Road, Hong Kong, China;* Email: yangdan@hku.hk

Authors

Fang-Fang Shen – *Morningside Laboratory for Chemical Biology, Department of Chemistry, The University of Hong Kong, Pokfulam Road, Hong Kong, China*

Sheng-Yao Dai – *Morningside Laboratory for Chemical Biology, Department of Chemistry, The University of Hong Kong, Pokfulam Road, Hong Kong, China*

Nai-Kei Wong – *Morningside Laboratory for Chemical Biology, Department of Chemistry, The University of Hong Kong, Pokfulam Road, Hong Kong, China; Department of Infectious Diseases, Shenzhen Third People's Hospital, The Second Hospital Affiliated to Southern University of Science and Technology, Shenzhen 518112, China*

Shan Deng – *School of Biological Sciences, The University of Hong Kong, Pokfulam Road, Hong Kong, China; Morningside Laboratory for Chemical Biology, Department of Chemistry, The University of Hong Kong, Pokfulam Road, Hong Kong, China*

Alice Sze-Tsai Wong – *School of Biological Sciences, The University of Hong Kong, Pokfulam Road, Hong Kong, China*

Notes

The results reported in this manuscript was filed in a U.S. provisional pat. Ser. No. 62/940,601, Nov 2019, by D.Y. and F.F.S.

ACKNOWLEDGMENT

We acknowledge support from The University of Hong Kong, Morningside Foundation, and the Hong Kong Research Grants Council under Collaborative Research Fund Scheme (HKU8CRF10) and the Area of Excellence Scheme (AoE/P-705/16). We thank Dr. Cheng Xu for the help in testing OCR by Seahorse instrument. We thank The University of Hong Kong Li Ka Shing Faculty of Medicine Faculty Core Facility for support in confocal microscopy and flow cytometry.

REFERENCES

1. Gouaux, E.; MacKinnon, R., Principles of Selective Ion Transport in Channels and Pumps. *Science* **2005**, *310*, 1461-1465.
2. Muraglia, K. A.; Chorghade, R. S.; Kim, B. R.; Tang, X. X.; Shah, V. S.; Grillo, A. S.; Daniels, P. N.; Cioffi, A. G.; Karp, P. H.; Zhu, L.; Welsh, M. J.; Burke, M. D., Small-molecule ion channels increase host defences in cystic fibrosis airway epithelia. *Nature* **2019**, *567*, 405-408.
3. Grillo, A. S.; SantaMaria, A. M.; Kafina, M. D.; Cioffi, A. G.; Huston, N. C.; Han, M.; Seo, Y. A.; Yien, Y. Y.; Nardone, C.; Menon, A. V.; Fan, J.; Svoboda, D. C.; Anderson, J. B.; Hong, J. D.; Nicolau, B. G.; Subedi, K.; Gewirth, A. A.; Wessling-Resnick, M.; Kim, J.; Paw, B. H.; Burke, M. D., Restored iron transport by a small molecule promotes absorption and hemoglobinization in animals. *Science* **2017**, *356*, 608-616.
4. Li, H.; Valkenier, H.; Judd, L. W.; Brotherhood, P. R.; Hussain, S.; Cooper, J. A.; Jurcek, O.; Sparkes, H. A.; Sheppard, D. N.; Davis, A. P., Efficient, non-toxic anion transport by synthetic carriers in cells and epithelia. *Nat. Chem.* **2016**, *8*, 24-32.
5. Liu, P. Y.; Li, S. T.; Shen, F. F.; Ko, W. H.; Yao, X. Q.; Yang, D., A small synthetic molecule functions as a chloride-bicarbonate dual-transporter and induces chloride secretion in cells. *Chem. Commun.* **2016**, *52*, 7380-3.
6. Ko, S.-K.; Kim, S. K.; Share, A.; Lynch, V. M.; Park, J.; Namkung, W.; Van Rossom, W.; Busschaert, N.; Gale, P. A.; Sessler, J. L.; Shin, I., Synthetic ion transporters can induce apoptosis by facilitating chloride anion transport into cells. *Nat. Chem.* **2014**, *6*, 885-892.
7. Busschaert, N.; Park, S.-H.; Baek, K.-H.; Choi, Y. P.; Park, J.; Howe, E. N. W.; Hiscock, J. R.; Karagiannidis, L. E.; Marques, I.; Félix, V.; Namkung, W.; Sessler, J. L.; Gale, P. A.; Shin, I., A synthetic ion transporter that disrupts autophagy and induces apoptosis by perturbing cellular chloride concentrations. *Nat. Chem.* **2017**, *9*, 667.
8. Huczyński, A., Polyether ionophores—promising bioactive molecules for cancer therapy. *Bioorg. Med. Chem. Lett.* **2012**, *22*, 7002-7010.
9. Sundelacruz, S.; Levin, M.; Kaplan, D. L., Role of membrane potential in the regulation of cell proliferation and differentiation. *Stem Cell Rev* **2009**, *5*, 231-46.
10. MacKinnon, R., Potassium Channels and the Atomic Basis of Selective Ion Conduction (Nobel Lecture). *Angew. Chem. Int. Ed.* **2004**, *43*, 4265-4277.
11. Xu, H.; Martinoia, E.; Szabo, I., Organellar channels and transporters. *Cell Calcium* **2015**, *58*, 1-10.
12. Garlid, K. D.; Paucek, P., Mitochondrial potassium transport: the K^+ cycle. *Biochim. Biophys. Acta* **2003**, *1606*, 23-41.
13. Shieh, C.-C.; Coghlan, M.; Sullivan, J. P.; Gopalakrishna, M., Potassium Channels: Molecular Defects, Diseases, and Therapeutic Opportunities. *Pharmacol. Rev.* **2000**, *52*, 557 – 593.
14. Prevarskaya, N.; Skryma, R.; Shuba, Y., Ion channels and the hallmarks of cancer. *Trends Mol. Med.* **2010**, *16*, 107-21.
15. Kim, H. K.; Noh, Y. H.; Nilius, B.; Ko, K. S.; Rhee, B. D.; Kim, N.; Han, J., Current and upcoming mitochondrial targets for cancer therapy. *Semin. Cancer Biol.* **2017**, *47*, 154-167.
16. Sancho, P.; Barneda, D.; Heeschen, C., Hallmarks of cancer stem cell metabolism. *Br. J. Cancer* **2016**, *114*, 1305-12.
17. Bonnet, S.; Archer, S. L.; Allalunis-Turner, J.; Haromy, A.; Beaulieu, C.; Thompson, R.; Lee, C. T.; Lopaschuk, G. D.; Puttagunta, L.; Bonnet, S.; Harry, G.; Hashimoto, K.; Porter, C. J.; Andrade, M. A.; Thebaud, B.; Michelakis, E. D., A mitochondria-

K^+ channel axis is suppressed in cancer and its normalization promotes apoptosis and inhibits cancer growth. *Cancer Cell* **2007**, *11*, 37-51.
18. Sisson, A. L.; Shah, M. R.; Bhosale, S.; Matile, S., Synthetic ion channels and pores (2004-2005). *Chem. Soc. Rev.* **2006**, *35*, 1269-1286.
19. Gokel, G. W.; Negin, S., Synthetic Ion Channels: From Pores to Biological Applications. *Acc. Chem. Res.* **2013**, *46*, 2824-2833.
20. Ren, C.; Chen, F.; Ye, R.; Ong, Y. S.; Lu, H.; Lee, S. S.; Ying, J. Y.; Zeng, H., Molecular Swings as Highly Active Ion Transporters. *Angew. Chem. Int. Ed.* **2019**, *58*, 8034-8038.
21. Ye, R.; Ren, C.; Shen, J.; Li, N.; Chen, F.; Roy, A.; Zeng, H., Molecular Ion Fishers as Highly Active and Exceptionally Selective K^+ Transporters. *J. Am. Chem. Soc.* **2019**, *141*, 9788-9792.
22. Yang, D.; Qu, J.; Li, B.; Ng, F.-F.; Wang, X.-C.; Cheung, K.-K.; Wang, D.-P.; Wu, Y.-D., Novel Turns and Helices in Peptides of Chiral α-Aminoxy Acids. *J. Am. Chem. Soc.* **1999**, *121*, 589-590.
23. Li, X.; Shen, B.; Yao, X.-Q.; Yang, D., A Small Synthetic Molecule Forms Chloride Channels to Mediate Chloride Transport across Cell Membranes. *J. Am. Chem. Soc.* **2007**, *129*, 7264-7265.
24. Zha, H.-Y.; Shen, B.; Yau, K.-H.; Li, S.-T.; Yao, X.-Q.; Yang, D., A small synthetic molecule forms selective potassium channels to regulate cell membrane potential and blood vessel tone. *Org. Biomol. Chem.* **2014**, *12*, 8174-8179.
25. Davis, J. T.; Gale, P. A.; Okunola, O. A.; Prados, P.; Iglesias-Sanchez, J. C.; Torroba, T.; Quesada, R., Using small molecules to facilitate exchange of bicarbonate and chloride anions across liposomal membranes. *Nat. Chem.* **2009**, *1*, 138-44.
26. Tetko, I. V.; Gasteiger, J.; Todeschini, R.; Mauri, A.; Livingstone, D.; Ertl, P.; Palyulin, V. A.; Radchenko, E. V.; Zefirov, N. S.; Makarenko, A. S.; Tanchuk, V. Y.; Prokopenko, V. V., Virtual Computational Chemistry Laboratory – Design and Description. *J. Comput. Aided Mol. Des.* **2005**, *19*, 453-463.
27. Busschaert, N.; Wenzel, M.; Light, M. E.; Iglesias-Hernández, P.; Pérez-Tomás, R.; Gale, P. A., Structure – Activity Relationships in Tripodal Transmembrane Anion Transporters: The Effect of Fluorination. *J. Am. Chem. Soc.* **2011**, *133*, 14136-14148.
28. Yang, D.; Li, B.; Ng, F.-F.; Yan, Y.-L.; Qu, J.; Wu, Y.-D., Synthesis and Characterization of Chiral N−O Turns Induced by α-Aminoxy Acids. *J. Org. Chem.* **2001**, *66*, 7303-7312.
29. Li, X.; Wu, Y.-D.; Yang, D., α-Aminoxy Acids: New Possibilities from Foldamers to Anion Receptors and Channels. *Acc. Chem. Res.* **2008**, *41*, 1428-1438.
30. Riddell, F. G.; Arumugam, S.; Brophy, P. J.; Cox, B. G.; Payne, M. C. H.; Southon, T. E., The nigericin-mediated transport of sodium and potassium ions through phospholipid bilayers studied by sodium-23 and potassium-39 NMR spectroscopy. *J. Am. Chem. Soc.* **1988**, *110*, 734-738.
31. Eisenman, G.; Horn, R., Ionic selectivity revisited: The role of kinetic and equilibrium processes in ion permeation through channels. *J. Membr. Biol.* **1983**, *76*, 197-225.
32. Gilles, A.; Barboiu, M., Highly Selective Artificial K^+ Channels: An Example of Selectivity-Induced Transmembrane Potential. *J. Am. Chem. Soc.* **2016**, *138*, 426-32.
33. Matile, S.; Sakai, N., The Characterization of Synthetic Ion Channels and Pores. In *Analytical Methods in Supramolecular Chemistry*, Wiley-VCH Verlag GmbH & Co. KGaA: 2007; pp 391-418.
34. Casey, J. R.; Grinstein, S.; Orlowski, J., Sensors and regulators of intracellular pH. *Nat. Rev. Mol. Cell Biol* **2009**, *11*, 50.
35. Poburko, D.; Santo-Domingo, J.; Demaurex, N., Dynamic regulation of the mitochondrial proton gradient during cytosolic calcium elevations. *J. Biol. Chem.* **2011**, *286*, 11672-84.
36. Kong, X.; Su, F.; Zhang, L.; Yaron, J.; Lee, F.; Shi, Z.; Tian, Y.; Meldrum, D. R., A Highly Selective Mitochondria-Targeting Fluorescent K^+ Sensor. *Angew. Chem. Int. Ed.* **2015**, *54*, 12053-12057.
37. Szewczyk, A.; Jarmuszkiewicz, W.; Kunz, W. S., Mitochondrial potassium channels. *IUBMB Life* **2009**, *61*, 134-43.
38. Zorov, D. B.; Juhaszova, M.; Sollott, S. J., Mitochondrial Reactive Oxygen Species (ROS) and ROS-Induced ROS Release. *Physiol. Rev.* **2014**, *94*, 909-950.
39. Yang, D., Wong, N. and Hu, J. (2018). US20150219676A1.
40. Manago, A.; Leanza, L.; Carraretto, L.; Sassi, N.; Grancara, S.; Quintana-Cabrera, R.; Trimarco, V.; Toninello, A.; Scorrano, L.; Trentin, L.; Semenzato, G.; Gulbins, E.; Zoratti, M.; Szabo, I., Early effects of the antineoplastic agent salinomycin on mitochondrial function. *Cell Death Dis.* **2015**, *6*, e1930.
41. Clevers, H., The cancer stem cell: premises, promises and challenges. *Nat. Med.* **2011**, 313.
42. Medema, J. P., Cancer stem cells: the challenges ahead. *Nat. Cell Biol.* **2013**, *15*, 338-44.
43. Frank, N. Y.; Schatton, T.; Frank, M. H., The therapeutic promise of the cancer stem cell concept. *J. Clin. Investig* **2010**, *120*, 41-50.
44. De Francesco, E. M.; Sotgia, F.; Lisanti, M. P., Cancer stem cells (CSCs): metabolic strategies for their identification and eradication. *The Biochemical journal* **2018**, *475*, 1611-1634.
45. Gupta, P. B.; Onder, T. T.; Jiang, G.; Tao, K.; Kuperwasser, C.; Weinberg, R. A.; Lander, E. S., Identification of selective inhibitors of cancer stem cells by high-throughput screening. *Cell* **2009**, *138*, 645-59.
46. Naujokat, C.; Steinhart, R., Salinomycin as a drug for targeting human cancer stem cells. *J. Biomed. Biotechnol.* **2012**, *2012*, 950658.
47. Boesch, M.; Zeimet, A. G.; Rumpold, H.; Gastl, G.; Sopper, S.; Wolf, D., Drug Transporter-Mediated Protection of Cancer Stem Cells From Ionophore Antibiotics. *Stem Cells Transl. Med.* **2015**, *4*, 1028-1032.
48. Boesch, M.; Sopper, S.; Wolf, D., Ionophore Antibiotics as Cancer Stem Cell-Selective Drugs: Open Questions. *Oncologist* **2016**, *21*, 1291-1293.
49. Chau, W. K.; Ip, C. K.; Mak, A. S. C.; Lai, H. C.; Wong, A. S. T., c-Kit mediates chemoresistance and tumor-initiating capacity of ovarian cancer cells through activation of Wnt/β-catenin – ATP-binding cassette G2 signaling. *Oncogene* **2012**, *32*, 2767.
50. Kryczek, I.; Liu, S.; Roh, M.; Vatan, L.; Szeliga, W.; Wei, S.; Banerjee, M.; Mao, Y.; Kotarski, J.; Wicha, M. S.; Liu, R.; Zou, W., Expression of aldehyde dehydrogenase and CD133 defines ovarian cancer stem cells. *Int. J. Cancer* **2012**, *130*, 29-39.
51. Farnie, G.; Sotgia, F.; Lisanti, M. P., High mitochondrial mass identifies a sub-population of stem-like cancer cells that are chemo-resistant. *Oncotarget* **2015**, *6*, 30472-30486.
52. Kim, H. K.; Noh, Y. H.; Nilius, B.; Ko, K. S.; Rhee, B. D.; Kim, N.; Han, J., Current and upcoming mitochondrial targets for cancer therapy. *Semin. Cancer Biol.* **2017**, *47*, 154-167.
53. Li, J.; Yuan, J., Caspases in apoptosis and beyond. *Oncogene* **2008**, *27*, 6194.
54. Elmore, S., Apoptosis: a review of programmed cell death. *Toxicol. Pathol.* **2007**, *35*, 495-516.
55. Vives-Bauza, C.; Zhou, C.; Huang, Y.; Cui, M.; de Vries, R. L.; Kim, J.; May, J.; Tocilescu, M. A.; Liu, W.; Ko, H. S.; Magrane, J.; Moore, D. J.; Dawson, V. L.; Grailhe, R.; Dawson, T. M.; Li, C.; Tieu, K.; Przedborski, S., PINK1-dependent recruitment of

Parkin to mitochondria in mitophagy. *Proc. Natl. Acad. Sci. U. S. A.* **2010**, *107*, 378-83.
56. Youle, R. J.; Narendra, D. P., Mechanisms of mitophagy. *Nature reviews. Molecular cell biology* **2011**, *12*, 9-14.
57. Kawai, A.; Uchiyama, H.; Takano, S.; Nakamura, N.; Ohkuma, S., Autophagosome-Lysosome Fusion Depends on the pH in Acidic Compartments in CHO Cells. *Autophagy* **2007**, *3*, 154-157.
58. Alfonso, I.; Quesada, R., Biological activity of synthetic ionophores: ion transporters as prospective drugs? *Chem. Sci* **2013**, *4*, 3009-3019.
59. Song, I. S.; Jeong, J. Y.; Jeong, S. H.; Kim, H. K.; Ko, K. S.; Rhee, B. D.; Kim, N.; Han, J., Mitochondria as therapeutic targets for cancer stem cells. *World J. Stem Cells* **2015**, *7*, 418-27.
60. Nazio, F.; Bordi, M.; Cianfanelli, V.; Locatelli, F.; Cecconi, F., Autophagy and cancer stem cells: molecular mechanisms and therapeutic applications. *Cell Death Differ.* **2019**, *26*, 690-702.
61. Lu, D.; Choi, M. Y.; Yu, J.; Castro, J. E.; Kipps, T. J.; Carson, D. A., Salinomycin inhibits Wnt signaling and selectively induces apoptosis in chronic lymphocytic leukemia cells. *Proc. Natl. Acad. Sci. U. S. A.* **2011**, *108*, 13253-7.
62. Mai, T. T.; Hamaï, A.; Hienzsch, A.; Cañeque, T.; Müller, S.; Wicinski, J.; Cabaud, O.; Leroy, C.; David, A.; Acevedo, V.; Ryo, A.; Ginestier, C.; Birnbaum, D.; Charafe-Jauffret, E.; Codogno, P.; Mehrpour, M.; Rodriguez, R., Salinomycin kills cancer stem cells by sequestering iron in lysosomes. *Nat. Chem.* **2017**, *9*, 1025 – 1033.
63. Huang, X.; Borgström, B.; Stegmayr, J.; Abassi, Y.; Kruszyk, M.; Leffler, H.; Persson, L.; Albinsson, S.; Massoumi, R.; Scheblykin, I. G.; Hegardt, C.; Oredsson, S.; Strand, D., The Molecular Basis for Inhibition of Stemlike Cancer Cells by Salinomycin. *ACS Central Science* **2018**, *4*, 760-767.
64. Wang, F.; Zhou, S.; Qi, D.; Xiang, S.-H.; Wong, E. T.; Wang, X.; Fonkem, E.; Hsieh, T.-c.; Yang, J.; Kirmani, B.; Shabb, J. B.; Wu, J. M.; Wu, M.; Huang, J. H.; Yu, W.-H.; Wu, E., Nucleolin Is a Functional Binding Protein for Salinomycin in Neuroblastoma Stem Cells. *J. Am. Chem. Soc.* **2019**, *141*, 3613-3622.
65. Kim, D. S.; Sessler, J. L., Calix[4]pyrroles: versatile molecular containers with ion transport, recognition, and molecular switching functions. *Chem. Soc. Rev.* **2015**, *44*, 532-46.
66. Sathiyajith, C.; Shaikh, R. R.; Han, Q.; Zhang, Y.; Meguellati, K.; Yang, Y. W., Biological and related applications of pillar[n]arenes. *Chem. Commun.* **2017**, *53*, 677-696.
67. Matile, S.; Som, A.; Sordé, N., Recent synthetic ion channels and pores. *Tetrahedron* **2004**, *60*, 6405-6435.
68. Montenegro, J.; Ghadiri, M. R.; Granja, J. R., Ion Channel Models Based on Self-Assembling Cyclic Peptide Nanotubes. *Acc. Chem. Res.* **2013**, *46*, 2955-2965.
69. Ren, C.; Shen, J.; Zeng, H., Combinatorial Evolution of Fast-Conducting Highly Selective K^+-Channels via Modularly Tunable Directional Assembly of Crown Ethers. *J. Am. Chem. Soc.* **2017**, *139*, 12338-12341.
70. Dworakowska, B.; Dołowy, K., Ion channels-related diseases. *Acta Biochim. Pol.* **2000**, *47*, 685-703.

For Table of Contents Only